# Critical Dynamics in the Presence of a Silica Gel

B. J. Frisken and David S. Cannell
*Department of Physics, University of California, Santa Barbara, California 93106*

(Received 30 April 1992)

Dynamic and static light scattering results are reported for isobutyric acid and water in a 4 wt.% silica network with a crossover length of 300 Å. In the one-phase region, well away from the critical point, the decay rate for order parameter fluctuations is unaffected by the network. Near the critical point, the order-parameter correlation function is well fitted by the sum of an exponential with decay rate $\Gamma_1$ and a term of the form $\exp[\ln(\tau/t_0)/\ln(\Gamma_2 t_0)]^3$, with $\Gamma_2 \simeq \Gamma_1$. When the system reaches conditions where the correlation length of the pure system is $\sim 100$ Å, it spontaneously orders.

PACS numbers: 64.70.Ja, 64.60.Ht, 68.45.Gd

In recent years, a number of investigations of the influence of quenched disorder on phase transitions have been carried out. Magnetic systems [1,2] have shown both altered critical behavior and extreme critical slowing down. Studies of gas-liquid [3] and binary-liquid [4-6] phase transitions, with disorder imposed by means of a porous glass or a percolating network (a gel), reveal some of these features, but it is not clear that these systems are described by the random-field Ising model [7,8]. For fluid systems, the order parameter (density or concentration, respectively) is conserved, while for magnetic systems it is not.

Here we report a detailed light scattering study of the isobutyric acid (IBA) and water system in the presence of a dilute (0.0186 vol.%), rigid, silica network, which imposes a spatially correlated field on the critical mixture. We observe that the order-parameter dynamics exhibit exponential relaxation with a decay rate equal to that of the pure IBA/water system for large enough values of the reduced temperature $t=(T-T_c)/T_c$, where $T_c$ refers to the pure system. The dynamics cross over to the sum of an exponential and an activated term upon decreasing $t$. The activated term is most significant at larger values of the scattering wave vector $q$, with the dynamics remaining exponential and diffusive at sufficiently small $q$. These observations are consistent with the predictions of Huse for the random-field Ising system with conserved order parameter [9]. However, upon reducing $t$ to $\sim 2\times10^{-3}$, the system spontaneously orders. This behavior is not predicted by theory to our knowledge. The ordering process is accompanied by the appearance of a very long time scale in the dynamics ($\sim 10$ s). This effect is transient and dies away over hours as the ordering proceeds. Examples of intensity-intensity correlation functions measured in each of the three dynamic regimes are shown in Fig. 1.

These studies have focused on rigid gels containing 4 wt.% silica which were grown by polymerization of tetramethylorthosilicate in water and were never dried [10]. These gels behave like mass fractals, with fractal dimension $D_f \simeq 2.2$, at length scales smaller than a crossover length $\xi_x \simeq 300$ Å. They are characterized [10] by a density-density correlation function given by $\langle\delta\phi_s(\mathbf{0}) \times\delta\phi_s(\mathbf{r})\rangle = 1.8\phi_s^2 e^{-r/\xi_x}/(r/\xi_x)^{3-D_f}$, where $\phi_s$ is the silica volume fraction and $\delta\phi_s$ is its deviation from the average. The gels were grown in 9.9 mm inner diameter glass tubes and were about 10 mm in length. After the gels had aged for more than 10 times their gelation time, they were exposed to IBA/water mixtures spanning the critical concentration of 39 wt.% IBA at a temperature of 40 °C, well above the critical temperature $T_c$. The supernatant was mixed daily and replaced once a week for $\sim 4$ weeks. After equilibration, the mixture above the gels was poured off so that the average concentration of the mix-

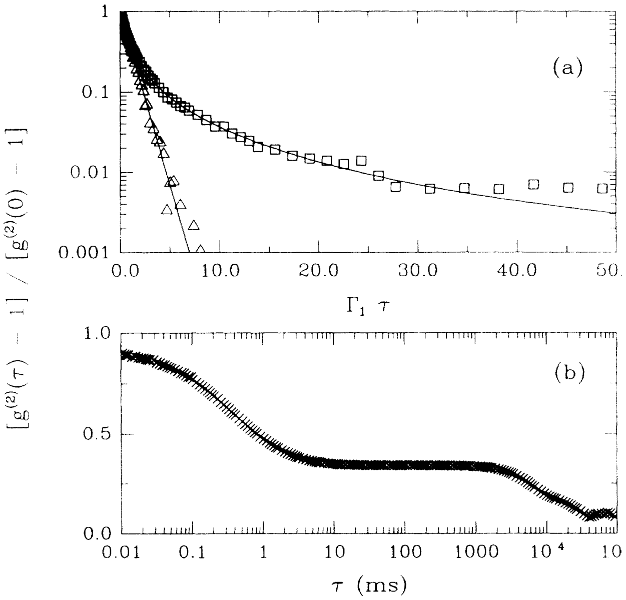

FIG. 1. Time correlation functions representative of the three dynamic regimes, measured at $q=1.9\times10^5\ \mathrm{cm}^{-1}$, in a sample containing 28 wt.% IBA at various temperatures. (a) The triangles show exponential data taken at 40 °C, and the squares show nonexponential data taken at 27.2 °C. The solid curves show fits by Eqs. (1) and (3). The delay time $\tau$ is scaled by the decay rate $\Gamma_1$. (b) The crosses are data taken at 27.05 °C, and show the additional slow dynamics representative of the third regime.

ture inside the gel could not change during the measurements. After the light scattering studies were complete, the concentration of the IBA relative to water in the gels was measured with an accuracy of ±1 wt.% by gas chromatography.

Before commencing studies of the gel-mixture samples, measurements were made to characterize the effect of concentration on critical phenomena in pure mixtures of 29, 34, 39, 44, and 49 wt.% IBA. The samples were contained in a water bath controlled to 1 mK. Measurements [11] of the total scattered intensity and its angular distribution (static measurements) determined the susceptibility and correlation length of the order-parameter fluctuations as a function of temperature and concentration. Measurements of the time dependence of the scattered light (dynamic measurements) determined the associated decay rates and diffusion coefficients. The critical temperature and correlation length amplitude were 26.67 °C and 3.61 Å, respectively.

We focused on gel-mixture samples containing 27, 28, and 30 wt.% IBA. As the critical region was approached, we found that the scattered intensity initially *decreased,* which indicates that the lower refractive index component (water) is preferentially adsorbed by silica. Further adsorption resulted in increased scattering. At the minimum, the gel was effectively masked, and the scattered intensity was approximately that of a pure IBA/water sample. This relatively weak scattering had two advantages: The samples did not scatter strongly enough to exhibit double scattering, and the dynamics of the spontaneous order-parameter fluctuations could be studied, despite strong preferential adsorption.

Under these conditions, the amplitude of the scattered electric field $E(t)$ consists of both a static and a zero-mean fluctuating component, $E_s$ and $E_f(t)$, respectively, where we associate $E_f(t)$ with time-dependent order-parameter fluctuations. The intensity-intensity correlation function $g^{(2)}(\tau)=\langle I(t)I(t+\tau)\rangle/\langle I(t)\rangle^2$ thus contains a cross term,

$$g^{(2)}(\tau)=1+\frac{2I_s\langle I_f\rangle}{\langle I(t)\rangle^2}g^{(1)}(\tau)+\frac{\langle I_f\rangle^2}{\langle I(t)\rangle^2}[g^{(1)}(\tau)]^2. \qquad (1)$$

Here $\langle I_f\rangle=\langle E_f(t)E_f^*(t)\rangle$, $I_s=E_sE_s^*$, and $\langle I(t)\rangle=\langle E(t)\times E^*(t)\rangle$, where the angular brackets denote time averaging, and $g^{(1)}(\tau)=\langle E_f(t)E_f^*(t+\tau)\rangle/\langle I_f\rangle$. Physically, the term linear in $g^{(1)}$ is the result of the time-dependent field beating with the time-independent field (heterodyne term) while the $[g^{(1)}]^2$ term is the result of it beating with itself (homodyne term). Equation (1) assumes both perfect alignment between the wave fronts of the static and fluctuating fields and detection at a single point in the scattered field. Aiming to approach this limit experimentally, we restricted our acceptance solid angle to the point where the correlation function for the pure system had an amplitude of 0.8 times the infinite delay value. We typically measured ten correlation functions with the sample clamped in different orientations and averaged the results of the fits. We also found that accurate data could be obtained by rotating the gel while measuring the correlation function, provided the rotation rate was sufficiently low [12].

Our data are consistent with two forms of $g^{(1)}(\tau)$,

$$g^{(1)}(\tau)=A_1e^{-\Gamma_1\tau}+A_2e^{(-\Gamma_2\tau)^x} \qquad (2)$$

or

$$g^{(1)}(\tau)=A_1e^{-\Gamma_1\tau}+A_2e^{[\ln(\tau/t_0)/\ln(\Gamma_2 t_0)]^3}. \qquad (3)$$

The first form includes a stretched exponential [13], and the second term of Eq. (3) is predicted by activated dynamic scaling theory [9,14] and has been used to fit Monte Carlo simulations of random-field systems [15] and light scattering data of binary fluids in Vycor [5]. Both forms fitted well and gave consistent results for the parameters $A_1$, $A_2$, $\Gamma_1$, and $\Gamma_2$, but the second typically gave a smaller $\chi^2$; the results of this fit will be reported here.

Figure 2 shows fitted results for the 28 wt.% IBA sample at a temperature of 27.2 °C. Figure 2(a) shows the amplitude of the activated term relative to the total amplitude as a function of $q$. Well above $T_c$, we found $A_2\simeq 0$, while near $T_c$, $A_2$ increased, becoming larger at large $q$ with a slight maximum versus $q$. This figure depicts the largest relative amplitude observed; maximum relative amplitudes measured in samples containing 27

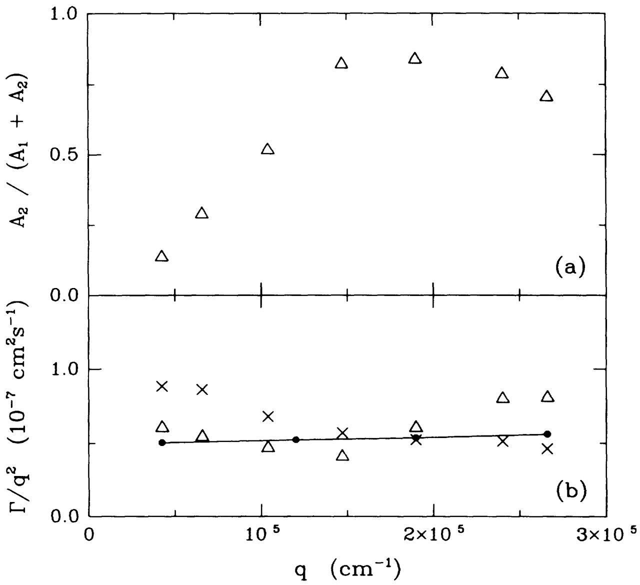

FIG. 2. Results of fitting nonexponential data taken in the sample containing 28 wt.% IBA at 27.2 °C by Eqs. (1) and (3). The $q$ dependence of the relative amplitude of the nonexponential term is shown in (a) while (b) shows the $q$ dependence of the two decay rates, $\Gamma_1$ (△) and $\Gamma_2$ (×). In (b), the solid circles and line show results interpolated from data for the pure system.

and 30 wt.% IBA were 0.2 and 0.55, respectively. Figure 2(b) shows the corresponding decay rates $\Gamma_1$ and $\Gamma_2$. For all of the samples studied, these two decay rates were comparable for a given $q$ and $T$, with both $\Gamma_1$ and $\Gamma_2 \propto q^2$, indicating diffusive behavior. This behavior is at least partially consistent with theory for random-field dynamics in the presence of a conserved order parameter [9] which predicts that the dynamics should become activated at small length scales while remaining diffusive and exponential at large length scales.

We also compared fit results for $\langle I_f \rangle$ to the intensity scattered by the pure system, finding that the amplitude of the fluctuations is reduced. Naively, one might interpret this ratio as an estimate of the fraction of the sample's volume which is exhibiting normal critical fluctuations. This ratio was $q$ independent and equal to 0.8 at 40 °C, and decreased to as little as 0.2 as the critical point was approached.

To compare these results to those for the pure samples, we estimated the concentration of the fluid exhibiting fluctuations using measurements of the nonfluctuating portion of the total scattered intensity, $I_s$. We model the static response of the water concentration to fluctuations in the silica concentration by

$$\delta\phi_w(\mathbf{q}) = \alpha(\mathbf{q},T)\,\delta\phi_s(\mathbf{q})\,, \tag{4}$$

allowing $\alpha$ to depend on both $q$ and $T$. Here $\delta\phi_w$ and $\delta\phi_s$ refer to fluctuations in the water and silica volume fractions, respectively. The nonfluctuating component of the light scattered by the gel-mixture system $S_{\mathrm{gm}}$, relative to that of the gel-water system $S_{\mathrm{gw}}$, can then be written [6] as

$$\frac{S_{\mathrm{gm}}(q)}{S_{\mathrm{gw}}(q)} = \frac{(\epsilon_{\mathrm{gm}}+2)^4}{(\epsilon_{\mathrm{gw}}+2)^4}\left[\frac{(K_s - K_{\mathrm{IBA}}) + \alpha(q,T)(K_w - K_{\mathrm{IBA}})}{K_s - K_w}\right]^2, \tag{5}$$

where $K \equiv (\epsilon-1)/(\epsilon+2)$, the subscripts $s$, IBA, and $w$ refer to silica, isobutyric acid, and water, respectively, and $\epsilon_{\mathrm{gm}}$ and $\epsilon_{\mathrm{gw}}$ are the dielectric constants of the gel-mixture and gel-water systems. Using Eq. (5), we deduced $\alpha(q,T)$ directly from measurements of the total intensity and that of the fluctuating component, $I_f$. The total intensity measurements were made while rotating the samples, so as to average over the frozen fluctuations. Well above $T_c$, the angular dependence of the scattered intensity was the same as that of the bare gel ($\alpha$ independent of $q$), while closer to $T_c$, the scattering deviated from that of the bare gel, developing a larger asymmetry between scattering at small and large $q$ ($\alpha$ decreased $\leq 20\%$ with increasing $q$). We deduced the average concentration in the portion of the sample which was not immobilized (free fluid) through the relation [6]

$$\phi_w^f(T) = \bar{\phi}_w - \alpha(q \to 0, T)\bar{\phi}_s\,, \tag{6}$$

which is independent of the volume occupied by the adsorbed fluid or its concentration.

Figure 3 shows the effects of adsorption on the weight fraction of IBA in the free fluid; strong shifts of the concentration are evident as $T \to T_c$. The arrows indicate the average IBA concentration for each sample as measured by gas-phase chromatography. The pure system's coexistence curve [16], shifted upward to agree with our measurements of the critical temperature, is shown as the solid line. The symbols are coded to summarize the dynamic light scattering results. Open symbols represent exponential behavior, while the dotted symbols indicate nonexponential behavior. The solid symbols show the onset of slow transient dynamics upon cooling. The general behavior was similar for all three samples, and the lower onset of nonexponential behavior for the 28 wt.% sample may well be due to slight differences in the gels (it was made in a different batch). For the open and dotted symbols, the system relaxed monotonically to equilibrium on a time scale faster than that for temperature equilibration.

We now compare the $q$-averaged diffusion coefficients $(\Gamma_1/q^2)$ of all three samples to those of pure mixtures at

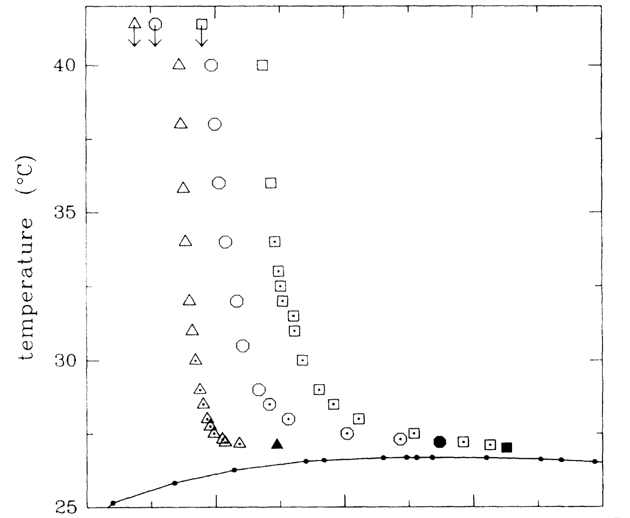

FIG. 3. Weight fraction of isobutyric acid in the *free fluid* determined using Eq. (6) for samples of 27 (△), 28 (○), and 30 (□) wt.% IBA. All of the gels are 4 wt.% silica with crossover lengths around 300 Å. The concentration of the free fluid is pulled dramatically towards the IBA-rich side. The solid curve is the pure system's coexistence curve shifted by +0.37 °C to agree with our measurements on pure samples, and the arrows show the average IBA concentration of each sample.

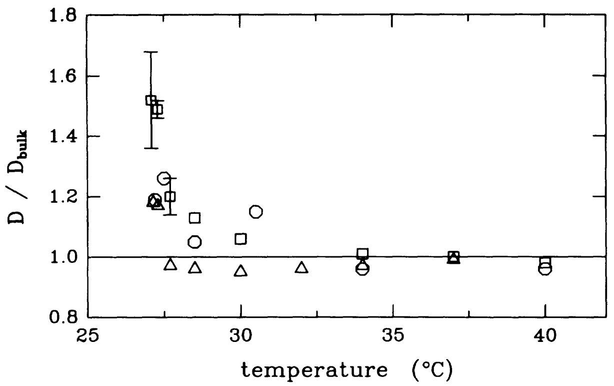

FIG. 4. The ratio of the diffusion coefficients for samples of 27 (△), 28 (○), and 30 (□) wt.% IBA to that of pure samples at the concentration of the free fluid, plotted as a function of temperature.

the same temperature and at the concentration estimated for the fluctuating fluid. These results are shown in Fig. 4. Throughout most of the first two dynamic regimes, the diffusion coefficients are nearly equal to those of a pure mixture of similar concentration and temperature, deviating significantly only at the lowest temperatures.

Upon further cooling, additional critical slowing down did not occur; instead, the correlation function abruptly developed a slow mode (decay time ~10 s) which appeared every time the sample temperature was lowered, and then slowly died away (over hours). This phenomenon was accompanied by overshoots [6] in the scattered intensity. For temperatures further than ~1 °C below the pure system's coexistence curve, this behavior ceased. It never appeared upon raising the temperature. No observable change in behavior occurred upon crossing the pure system's coexistence curve. We associate this slow mode with a phase-separation-like process, even though it began nearly 0.5 °C *above* the pure system's coexistence curve, well beyond what could be attributed to possible $T_c$ shifts from impurities. We speculate that when the concentration difference between the adsorbed fluid and that participating in critical fluctuations becomes large enough, and occurs over sufficiently short distances, the free energy cost due to gradient terms drives the system to segregate the free fluid into regions of below average silica concentration. Samples held in this two-phase region, either *above* or *below* the coexistence curve of the pure system, returned to their previous scattering values only over a period of days when the temperature was raised well into the one-phase region. This indicates that mass transport had occurred on macroscopic length scales, and that this system exhibits long-range order in three dimensions. However, the time scale for complete phase separation in the Earth's gravitational field could be very long.

We wish to thank Andrea Liu for helpful conversations. This research was supported by NSF Grant No. DMR 90-18089.

[1] See, for example, D. S. Fisher, G. M. Grinstein, and A. Khurana, Phys. Today **41**, No. 12, 56 (1988), and references therein.

[2] V. Jaccarino and A. R. King, Physica (Amsterdam) **163A**, 291 (1990).

[3] A. P. Y. Wong and M. H. W. Chan, Phys. Rev. Lett. **65**, 2567 (1990); A. P. Y. Wong, S. B. Kim, J. Ma, W. I. Goldburg, and M. H. W. Chan (unpublished).

[4] J. V. Maher, W. I. Goldburg, D. W. Pohl, and M. Lanz, Phys. Rev. Lett. **53**, 60 (1984); K.-Q. Xia and J. V. Maher, Phys. Rev. A **36**, 2432 (1987); **37**, 3626 (1988).

[5] S. B. Dierker and P. Wiltzius, Phys. Rev. Lett. **58**, 1865 (1987); P. Wiltzius, S. B. Dierker and B. S. Dennis, Phys. Rev. Lett. **62**, 804 (1989); S. B. Dierker and P. Wiltzius, Phys. Rev. Lett. **66**, 1185 (1991).

[6] B. J. Frisken, F. Ferri, and D. S. Cannell, Phys. Rev. Lett. **66**, 2754 (1991).

[7] A. J. Liu, D. J. Durian, E. Herbolzheimer, and S. A. Safran, Phys. Rev. Lett. **65**, 1897 (1990); (unpublished).

[8] A. Maritan, M. R. Swift, M. Cieplak, M. H. W. Chan, M. W. Cole, and J. R. Banavar, Phys. Rev. Lett. **67**, 1821 (1991).

[9] D. A. Huse, Phys. Rev. B **36**, 5383 (1987).

[10] F. Ferri, B. J. Frisken, and D. S. Cannell, Phys. Rev. Lett. **67**, 3626 (1991).

[11] H. R. Haller, C. Destor, and D. S. Cannell, Rev. Sci. Instrum. **54**, 973 (1983).

[12] B. J. Frisken and D. S. Cannell (to be published).

[13] See, for example, G. Williams, J. Non-Cryst. Solids **131**, 1 (1991).

[14] D. S. Fisher, Phys. Rev. Lett. **56**, 416 (1986).

[15] A. T. Ogielski and D. A. Huse, Phys. Rev. Lett. **56**, 1298 (1986).

[16] D. Woermann and W. Sarholz, Ber. Bunsenges. Phys. Chem. **69**, 319 (1965).